

## Aluminum extraction from a metallurgical industry sludge and its application as adsorbent

Juan C. Mahecha-Rivas<sup>a</sup>, Edwin Fuentes-Ordoñez<sup>b</sup>, Eva Epelde<sup>c</sup>, Juan F. Saldarriaga<sup>a,\*</sup>

<sup>a</sup>*Dept. Civil and Environmental Engineering, Universidad de los Andes, Bogotá, Colombia*

<sup>b</sup>*Nanomaterials and Computer Aided Process Engineering Research Group (NIPAC), Dept. Chemical Engineering, Faculty of Engineering, University of Cartagena, Av. del Consulado Calle 30 No. 48-152, Cartagena, Colombia*

<sup>c</sup>*Dept. Chemical Engineering, University of the Basque Country, Leioa, Spain.*  
*jf.saldarriga@uniandes.edu.co, juanfelorza@gmail.com*

### Abstract

The aluminum industry produces a high amount of wastes that are concentrated in the sludge of their water treatment plants. This sludge is rich in aluminum, which could be extracted and purified. In this work, three extraction methods have been evaluated to recover the aluminum from the sludge samples provided by a metallurgical industry from Medellín, Colombia. The sludge has been characterized to confirm its high aluminum content. The Bayer extraction method has been carried out, using 1:10, 1:15 and 1:20 sludge/solution mass ratios, and HCl extraction, by using 1:15 and 1:20 ratios. The extraction with isopropanol has also been evaluated. The amounts of Al, Fe, Cu, and Ni present in the aqueous phase have been measured to determine the recovery of the metals, as well as the selectivity of the extraction method. The highest metal recovery (99.3%) is achieved by HCl extraction for a sludge/solution ratio of 1:20, while the Bayer method (1:15 ratio) has shown the best selectivity. On the other hand, the extraction with isopropanol has not been successful for any of the ratios evaluated. The extracted material has been tested as an adsorbent for the removal of chlorpyrifos (200 mg/l), where the removal percentages have been higher than 95% for all the weight ratios studied. Hence, this Al-enriched material shows good prospects to be used as an adsorbent in the treatment of polluted water.

1  
2  
3  
4 28 *Keywords:* Aluminum extraction; sludge; Bayer process; isopropanol; hydrochloric acid;  
5  
6  
7 29 chlorpyrifos removal  
8  
9 30

## 11 31 **1. Introduction**

12 32 The aluminum industry is one of the most prosperous in recent years, being aluminum one  
13  
14 33 of the most widely used non-ferrous metals worldwide. Its production has increased in the  
15  
16 34 last decade from 37,606 thousand metric tonnes in 2009 to 63,697 thousand metric tonnes in  
17  
18 35 2019, showing a growth of 59% for this period [1]. The main applications include  
19  
20  
21 36 transportation, packaging, construction, and electrical engineering [2–4].  
22  
23  
24  
25

26 37 The extraction of aluminum from bauxite for the production of aluminum or alumina is  
27  
28 38 usually carried out by the Bayer process, which consists of the solubilization of the aluminum  
29  
30 39 species present in the bauxite in a hot solution of NaOH [5,6]. Aluminum reacts with the  
31  
32 40 solution to form sodium aluminate, a soluble compound that, when diluted and cooled,  
33  
34 41 precipitates as trihydrate alumina [5]. The precipitate is subsequently calcined to remove  
35  
36 42 moisture impurities to obtain the desired compound.  
37  
38  
39  
40

41 43 Although the Bayer process is widely used, high pressure and temperature conditions are  
42  
43 44 needed, giving way to high operating costs [7]. Additionally, some impurities (i.e. Na<sub>2</sub>O,  
44  
45 45 CaO, SiO<sub>2</sub>, MgO, Fe<sub>2</sub>O<sub>3</sub>, etc.) are usually present in the final product [8]. On the other hand,  
46  
47 46 extraction with HCl produces aluminum hydroxy chlorides (PACs), which, after additional  
48  
49 47 treatments, could be used as flocculants in water treatment or in the cosmetic industry [9].  
50  
51  
52 48 Extraction with isopropanol produces aluminum isopropoxide, a catalyst for reactions with  
53  
54 49 aldehydes [10] which can be transformed, with additional treatments, to aluminum  
55  
56 50 hydroxide, boehmite or pseudo-boehmite [7,9,11].  
57  
58  
59  
60  
61  
62  
63  
64  
65

1  
2  
3  
4 51 Once Al is extracted, the samples are subjected to different treatments, such as the anodizing  
5  
6 52 process, which provides anticorrosive protection, but generates sludges composed of high  
7  
8 53 alumina content and a variety of alkaline chemicals [2]. Anodized aluminum sludge is mainly  
9  
10 54 composed of aluminum hydroxide, oxide-aluminum hydroxide, and aluminum oxides [11–  
11  
12 55 13]. For every 1 tonne of anodized aluminum, 475 kg of sludge are generated, and it is  
13  
14 56 estimated that the countries of the EU produce about 100,000 metric tonnes per year [14,15].  
15  
16 57 The disposal of these wastes in specific sanitary fills is currently an environmental problem,  
17  
18 58 due to the high volume of wastes generated. Furthermore, transportation costs are estimated  
19  
20 59 in 22-30 US\$/tonne [15]. Attempts have been made to look for possible market applications  
21  
22 60 in the cement, ceramic, and/or paper industries. However, few industries are available, which  
23  
24 61 can only valorize ~20% of the overall waste generated [15].  
25  
26  
27  
28  
29  
30

31  
32 62 Aluminum hydroxide ( $\text{Al}(\text{OH})_3$ ) is used in refractory materials, ceramics, polishing and  
33  
34 63 abrasion applications, manufacture of zeolites, fire retardants and catalysts, among others  
35  
36 64 [16]. These applications are possible due to the high alumina content of the sludge, with a  
37  
38 65 composition almost constant over time, which makes its recycling process more attractive.  
39  
40 66 These sludges have also been used in various inert matrices, such as concrete, glass, and  
41  
42 67 ceramics [15,17].  
43  
44  
45  
46

47 68 This work aims to evaluate, by different extraction methods, the recovery of the aluminum  
48  
49 69 contained in a wastewater sludge derived from a metallurgical industry. For this purpose,  
50  
51 70 Bayer, HCl, and isopropanol extraction methods are compared for different reagent ratios.  
52  
53 71 Besides, the extracted product has been evaluated for its application as adsorbent for the  
54  
55 72 removal of an organophosphate pesticide (chlorpyrifos, CPS) from contaminated waters.  
56  
57  
58  
59  
60  
61  
62  
63  
64  
65

1  
2  
3  
4 73 Similarly, a model of adsorption isotherms has been carried out from the isotherms proposed  
5  
6  
7 74 by Langmuir and Freundlich.

## 9 75 **2. Experimental**

10 76 The treated sludge sample (20 kg) has been provided by a company located in Medellín  
11  
12 77 (Colombia), dedicated to the production of extraction, lamination, foil, and manufactured  
13  
14 78 pieces. The sludge comes from the wastewater treatment plant, which must be neutralized  
15  
16 79 before its disposal in a sanitary landfill. The sludge has been subjected to a mild drying  
17  
18 80 process for 48 h at 40 °C, so that the compounds contained would not degrade or react. The  
19  
20 81 dried sludge has been crushed with a RETSCH® A7304184 jaw crusher and then passed  
21  
22 82 through a 500 µm mesh screen.  
23  
24  
25  
26  
27  
28  
29

### 30 83 *2.1. Analytical methods*

31  
32  
33 84 The elemental analysis for the quantification of N, C, S, H, and O has been carried out  
34  
35 85 following the ASTM D5373-16 standard on the Elementar Vario Macro CHNS® (Elementar,  
36  
37 86 Langensfeld, Germany). Additionally, X-ray Fluorescence (FRX) analysis have been  
38  
39 87 performed on the raw sludge to identify and quantify the atomic species in a ZSX Primus  
40  
41 88 Rigaku® (Rigaku, Tokyo, Japan) spectrophotometer. Likewise, an XRD analysis with  
42  
43 89 Rigaku Ultima III (Rigaku, Tokyo, Japan) and SEM analysis were carried out through a  
44  
45 90 microscope TESCAN LYRA3 FIB-SEM (TESCAN, Brno, Czech Republic) for the three  
46  
47 91 samples, both the raw sludge, after being processed and when it was used as adsorbent.  
48  
49  
50  
51  
52

53 92 The quantification of metal concentration has been performed using inductively coupled  
54  
55 93 plasma optical emission spectrometry (ICP-OES) in an ICP-OES Thermo Scientific™  
56  
57 94 ICAP6500 DUO kit (Thermo Scientific, Waltham, MA, USA) equipment. The Al content of  
58  
59  
60  
61  
62  
63  
64  
65

1  
2  
3  
4 95 all the samples has been determined by this technique. Additionally, the samples derived  
5  
6 96 from Bayer and HCl extraction have been analyzed for Cu, Fe, and Ni. Due to the high  
7  
8  
9 97 volume of the samples taken, all of them underwent a 1:10 dilution before digestion. The  
10  
11 98 samples were digested following the EPA3015A standard [18] for liquid samples and  
12  
13 99 EPA3051A [19] for solid samples. The analytical method was applied following Standard  
14  
15  
16 100 Methods standard 3120B [20] for aqueous samples and EPA standard 6010C [21] for solid  
17  
18 101 samples. The measurement wavelength for aluminum was 308.2 nm. The physical properties  
19  
20  
21 102 of the extracted samples have been estimated by N<sub>2</sub> adsorption–desorption (Micromeritics  
22  
23 103 ASAP 2010) at -196 °C. The samples have been pretreated at 150 °C for 8 h under vacuum  
24  
25  
26 104 ( $10^{-3}$  mmHg), to remove possible impurities. The specific surface area ( $S_{\text{BET}}$ ) has been  
27  
28 105 calculated using the Brunauer, Emmett, Teller equation and the total pore volume ( $V_{\text{p}}$ ) is  
29  
30  
31 106 based on the Gurvitch rule (for relative pressure  $P/P_0 > 0.99$ ) [22,23]. The microporous  
32  
33 107 surface ( $S_{\text{micro}}$ ) and volume ( $V_{\text{micro}}$ ) have been calculated using the t-plot method and  
34  
35  
36 108 mesoporous volume ( $V_{\text{meso}}$ ) has been estimated by the difference between total and micropore  
37  
38 109 volume ( $V_{\text{meso}}=V_{\text{p}}-V_{\text{micro}}$ ). The pore size distributions have been determined by Barrer-  
39  
40 110 Joyner-Halenda (BJH) method. The acidity and acid strength of the catalysts were measured  
41  
42  
43 111 by monitoring the adsorption-desorption of NH<sub>3</sub> by combining the techniques of thermo-  
44  
45  
46 112 gravimetric analysis and the differential scanning calorimetry, using a Setaram TG-DSC  
47  
48 113 calorimeter connected online with a Thermostar mass spectrometer (Balzers Instruments)  
49  
50 114 following the procedure previously reported in [24].  
51

## 52 115 2.2. Procedure for extraction method

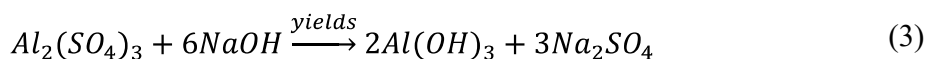
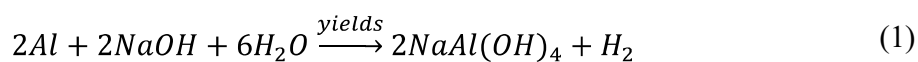
53  
54  
55  
56  
57  
58  
59  
60  
61  
62  
63  
64  
65

1  
2  
3  
4 116 For the three aluminum extraction methods the same assembly has been performed. The  
5  
6  
7 117 vessel consists of a 2-neck flask, one for the reflux condenser, and the other for the  
8  
9 118 thermometer or sampling, placed on a temperature-controlled heating blanket.

10  
11  
12 119 • *Bayer extraction process*

13  
14  
15 120 A NaOH (2M) solution has been used as the extraction substance. Three different tests have  
16  
17 121 been performed for different sludge/solution ratios and a control sample composed only of  
18  
19 122 the extraction solution has also been tested. In each test, 700 ml of the extraction solution is  
20  
21 123 added to the flask, together with a certain amount of sludge, 70.00 g, 46.67 g, and 35.00 g of  
22  
23 124 sludge corresponding to 1:10, 1:15 and 1:20 sludge/solution mass ratios, respectively [25,26].  
24  
25 125 These tests are based on the methodology proposed in the literature [27,28], to assure the  
26  
27 126 maximum recovery of aluminum. The mixtures have been brought to boiling point,  
28  
29 127 corresponding to zero time. 20 ml aliquots have been taken from the flask mixture every 30  
30  
31 128 min up to 3 h for the analysis of metal content (by ICP-EOS, Section 2.1). Aliquots have  
32  
33 129 been positive pressure filtered to remove solids.

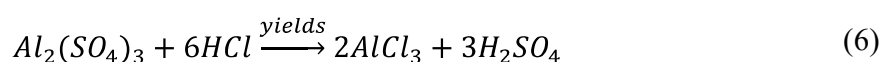
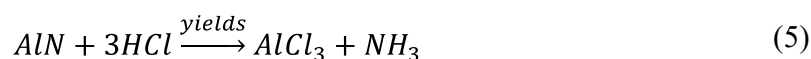
34  
35 130 It should be noted that the extraction of Al with NaOH in the aqueous phase involves a  
36  
37 131 chemical attack on only part of the Al species, probably present in the mud. Corundum and  
38  
39 132 spinel are not attacked by basic dissolution. Thus, the following reactions are likely to occur  
40  
41 133 during this extraction process [29]:



42  
43  
44  
45  
46  
47  
48  
49  
50  
51  
52  
53  
54  
55  
56  
57  
58  
59  
60 134  
61  
62  
63  
64  
65

135 • *HCl extraction process*

136 Acid extraction allows the recovery of Al from the same species mentioned in the basic  
 137 extraction, where it is suggested that the reactions that take place are as follows [30]:

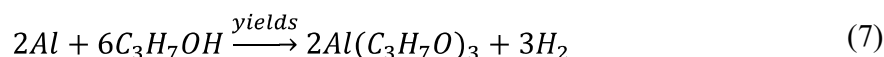


138

139 The same procedure followed for the Bayer extraction method has been carried out. In this  
 140 case, a 2M HCl solution has been used as the extraction substance. Two tests have been  
 141 carried out, by adding 700 ml of the extraction solution to the flask, and a quantity of sludge  
 142 determined by the ratio corresponding to the test: 46.67 g and 35.00 g of sludge,  
 143 corresponding to 1:15 and 1:20 ratios, respectively. The metal content has also been  
 144 determined by ICP-EOS (Section 2.1).

145 • *Extraction process with isopropanol*

146 The Al recovery with isopropanol can occur according to the following reaction [31,32]:



147

148 For this method, analytical grade isopropanol has been used as the extraction agent. The tests  
 149 have been carried out based on the procedure proposed by Saiz et al. [7]. This process aims  
 150 to obtain aluminum monohydroxide through the reaction between the sludge and the  
 151 isopropanol to produce aluminum isopropoxide (Eq. (7)),

152 The different extraction tests are summarized in Table 1. One of the tests corresponds to a  
 153 control sample in which aluminum has been used instead of the sludge. In each test, the  
 154 catalysts composed of sublimated iodine ( $I_2$ ), and mercury chloride ( $HgCl_2$ ), have been  
 155 dissolved in 50 ml of isopropanol at 70 °C. The sludge has been added to the flask, then the  
 156 isopropanol with the catalysts, and finally, the rest of the isopropanol. The mixture in the  
 157 flask has been brought to a boil at 75 °C (at 560 mmHg), corresponding to zero time.  
 158 According to Saiz et al. [7] the reaction time depends on the catalyst used. In this work, using  
 159  $I_2$  and  $HgCl_2$  catalysts, reaction times between 3 and 11 h have been established. After each  
 160 test, the content of the flask has been weighted, and the phases have been separated by  
 161 positive pressure filtration. Retroevaporation distillation of the aqueous phase has been  
 162 performed at 80 °C for 3 h to reduce the amount of isopropanol. Finally, a metal analysis has  
 163 been carried out on the aqueous phase of each test, as well as on the solid phase by ICP-EOS  
 164 (Section 2.1).

165 **Table 1.** List of reagents used in each isopropanol extraction test.

<b>Test</b>	<b>Control</b>		<b>Test 1</b>		<b>Test 2</b>	
<b>Time (h)</b>	7		3		3	
<b>Reagents/catalysts</b>	Ratio (mol/mol Al)	Weight (g)	Ratio (mol/mol Al)	Weight (g)	Ratio (mol/mol Al)	Weight (g)
<b>Sludge*</b>	-	11.80	-	16.76	-	18.78
<b>2-propanol**</b>	6.00	155.69	6.00	133.89	6.70	77.84
<b><math>I_2</math></b>	0.01	1.15	0.00	0.15	0.01	0.39
<b><math>HgCl_2</math></b>	0.03	3.67	0.00	0.00	0.00	0.00
<b>Sediment Measurement</b>	No		No		No	
<b>Test</b>	<b>Test 3</b>		<b>Test 4</b>		<b>Test 5</b>	
<b>Time (h)</b>	7		11		11	
<b>Reagents/catalysts</b>	Ratio (mol/mol Al)	Weight (g)	Ratio (mol/mol Al)	Weight (g)	Ratio (mol/mol Al)	Weight (g)



<b>Sludge*</b>	-	43.83	-	69.50	-	69.49
<b>2-propanol**</b>	6.00	155.69	3.60	155.69	3.60	155.69
<b>I<sub>2</sub></b>	0.01	1.11	0.00	0.18	0.01	1.19
<b>HgCl<sub>2</sub></b>	0.03	3.58	0.00	0.18	0.02	3.79

<b>Sediment Measurement</b>	No	Yes	Yes
-----------------------------	----	-----	-----

\* From the amount of the sludge the molar amount of A is calculated using the concentration characterization - ICP (Exception Test 1). \*\* The mass of 2-propanol is calculated from the added volume and the density of 2-propanol at 20 °C (0.786 g/ml).

166 • *Recovery fraction (RF)*

167 In this work to clearly observe the extraction force of each method, the concept of the  
168 recovery fraction (RF) is used, which is defined as the fraction of the aluminum extracted  
169 with respect to the initial quantity [33].

170 During the Bayer and HCl extractions, 20 ml aliquots were taken every 30 min and were  
171 analyzed by ICP-EOS (Section 2.1) to determine the metal content. For these cases, the RF  
172 is the mass found in the aqueous phase, which is the dissolved mass inside the flask plus the  
173 mass removed in the aliquots, over the initial mass of Al. It is expressed as shown in Eq. (8)  
174 and Eq. (9):

$$V_i = V_0 - V_{Al} \left( \frac{i}{30} \right) \quad (8)$$

$$RF_i = \left( \frac{1g}{1000mg} \right) \frac{[C_i V_i + V_{Al} \sum_{j=30}^{i-30} C_j]}{(C_{sludge} m_{sludge})} \quad (9)$$

175 where,  $i$ , is the sampling time ( $i = 0, 30, 60, 90, 120, 150, 180$  min);  $RF_i$ , is the recovery  
176 fraction at time  $i$  (-);  $C_i$ , the concentration of the aqueous phase at time  $i$  ( $mg\ l^{-1}$ );  $V_i$ , the  
177 volume in the flask at time  $i$  (l);  $V_0$ , initial volume ( $V_0 = 0.7$  l);  $V_{al}$ , aliquot volume ( $V_{al} = 0.02$   
178 l);  $C_{sludge}$ , initial sludge concentration ( $C_{sludge} = 27.8$  wt%);  $m_{sludge}$ , the initial sludge mass (g).

179 In the case of isopropanol extraction, aliquots have been only taken in the final aqueous  
180 solution. Therefore, RF can be defined by Eq. (10), as follows:

$$RF_i = \left( \frac{1g}{1000mg} \right) \left( \frac{C_i V_i + Vol \sum C_i}{C_{sludge} m_{sludge}} \right) \quad (10)$$

181 2.3. *Chlorpyrifos (CPS) adsorption tests*

182 CPS has been used as a reference water pollutant for the adsorption tests, due to its wide use  
 183 as a pesticide in agriculture, used indiscriminately especially in developing countries, such  
 184 as Colombia. Its inadequate management and wide use have affected runoff and ground  
 185 waters, generating health problems in the population. According to García-Reyes et al. [34]  
 186 and Sharma and Kakkar [35] the maximum permissible limits of individual and total pesticide  
 187 in drinking water are 0.1 and 0.5 ppb, respectively. For this study, a maximum pesticide  
 188 concentration of 200 mg l<sup>-1</sup> has been taken.

189 The adsorption tests have been carried out with different weights (0-5 g) of the precipitate  
 190 obtained from the Bayer extraction process for a ratio of 1:15 (BES15). To check for  
 191 reproducibility, all samples have been made in quadruplicate. The vials have been filled with  
 192 100 ml of the standard solution, the flasks have been shaken and the samples have been taken  
 193 at 5, 30, 60, 90, 120, 150, 180, 210, and 240 mins. The vials are placed in a SIF 3000 model  
 194 shaker (MAX QTM, Chandler, United States) at room temperature and 120 rpm. For lecture,  
 195 5 ml of the solution has been taken at each time and analyzed in a tube absorbance  
 196 spectrophotometer using a Thermo Spectrophotometer UV Genesys (Thermo Fisher  
 197 Scientific, Waltham, United States). Before analyses, calibration tests have been performed  
 198 following ASTM-D3860-98. The equipment has been calibrated at different wavelengths  
 199 with the problem solution. Similarly, the absorbance of the pollutant has been measured  
 200 keeping the value of the wavelength constant, for the 20 solutions prepared with

1  
2  
3  
4 201 concentrations from 0.5 to 400 mg l<sup>-1</sup> of chlorpyrifos. A slope of 0.0107, an intercept of  
5  
6 202 0.0286, and an R<sup>2</sup> of 0.9972 has been obtained.  
7

8  
9  
10 203 The most widely accepted models in the literature have been used to describe the adsorption  
11  
12 204 isotherms [36]: Langmuir, Eq. (11); and, Freundlich, Eq. (12):  
13  
14

$$q_e = \frac{Q_{max}^0 K_L C_e}{1 + K_L C_e} \quad (11)$$

$$q_e = K_F C_e^n \quad (12)$$

15  
16  
17  
18  
19  
20  
21 205 where  $Q_{max}^0$  (mg g<sup>-1</sup>) is the maximum saturated monolayer adsorption capacity of an  
22  
23 206 adsorbent,  $q_e$  (mg g<sup>-1</sup>) is the amount of adsorbate uptake at equilibrium,  $K_L$  (l mg<sup>-1</sup>) is the  
24  
25 207 constant related to the affinity between an adsorbent and adsorbate,  $C_e$  (mg l<sup>-1</sup>) is the  
26  
27 208 adsorbate concentration at equilibrium,  $K_F$  (mg g<sup>-1</sup>)/(mg l<sup>-1</sup>) is the Freundlich constant,  $n$  is  
28  
29 209 the Freundlich intensity parameter, which indicates the magnitude of the adsorption driving  
30  
31  
32  
33 210 [36–38].  
34  
35  
36

37 211 Langmuir's principle assumes that there is a fixed number of accessible sites that are available  
38  
39 212 on the surface of the adsorbent and that once the adsorbate occupies one site, no further  
40  
41 213 adsorption can occur at that site. While Freundlich cannot describe the linearity ratio at very  
42  
43 214 low concentrations nor the saturation effect at very high concentrations [39,40].  
44  
45  
46

47 215 Likewise, the adsorption kinetics, which represents the dynamics of the adsorption process,  
48  
49 216 have been analyzed by the mass balance of the adsorbate between the liquid and solid, and  
50  
51 217 are described as follows:  
52  
53  
54

$$q_t = q_e(1 - e^{-k_1 t}) \quad (13)$$

$$\frac{dc}{dt} = \frac{-k_1 a S (c - c_e)}{L} \quad (14)$$

$$\frac{dq}{dt} = k_L \alpha (c - c_e) \quad (15)$$

218 where  $q_e$  and  $q_t$  are the amounts of adsorbate uptake per mass of adsorbent at equilibrium and  
 219 at any time  $t$  (min), respectively, and  $k_1$  ( $\text{min}^{-1}$ ) is the rate constant of the pseudo-first-order  
 220 kinetic equation (PFO),  $k_L$  ( $\text{l m}^{-2} \text{min}^{-1}$ ) is the mass transfer coefficient,  $a$  ( $\text{m}^2 \text{g}^{-1}$ ) the external  
 221 surface area of adsorbent,  $L$  the volume of CPS solution and  $\rho_b$  ( $\text{kg m}^{-3}$ ) the adsorbent bed  
 222 density.  $k_1 a \rho_b$  represents the rate constant of the pseudo-first-order kinetic model.

223 The equilibrium parameters for the models of Freundlich and Langmuir, Eqs. (11) and (12),  
 224 have been optimized, by minimizing an objective function,  $OF$ , defined as the sum of the  
 225 squares of the differences between the values of the concentration of adsorbate in the liquid  
 226 phase measured experimentally,  $c_{exp}$ , and the values calculated by the model,  $c_{cal}$ . For this, a  
 227 calculation algorithm has been implemented in MATLAB, which uses the *ode* subroutine to  
 228 solve the mass balance equations, Eq. (12), and the *fminsearch* subroutine, which calculates  
 229 the without restrictions minimum of the objective function, based on the Nelder-Mead  
 230 algorithm.

### 231 3. Results and discussion

#### 232 3.1. Chemical characterization of the raw sludge

233 According to XRF results (Table S.1.), the content of Al (68.52%) outstands among other  
234 species, being the concentration levels similar to those found in other studies [3,41].  
235 Therefore, this sludge shows a high concentration of Al, which has a high potential to be  
236 extracted and with little interference with other metallic species. The high concentration of S  
237 (28 wt%) observed may be due to the neutralization treatments carried out in the company at  
238 its place of origin.

239 Therefore, an ICP-OES analysis has been carried out to determine the metal concentration  
240 present in the sample (Table S.1.). For this specific work, Na was not quantified, since the  
241 Bayer extraction is carried out with NaOH, so it would not be possible to compare the initial  
242 characterization with the results of the extractions, in the same way, Ca was not quantified.  
243 It has been found that the concentration of Al determined by XRF is higher than that  
244 determined by ICP since the XRF technique quantifies the total Al present in the mud. The  
245 composition of the sludge is complex. However, it can be suggested that the total Al is  
246 provided by species, such as metallic Al, aluminum nitride (AlN), aluminum sulfate  
247 ( $\text{Al}_2\text{SO}_4$ ), aluminum hydroxide ( $\text{Al}(\text{OH})_3$ ), aluminum oxides ( $\text{Al}_2\text{O}_3$ ) and spinel ( $\text{MgAl}_2\text{O}_4$ )  
248 [29,42]. On the other hand, the Al determined by ICP corresponds to the Al species soluble  
249 in aqueous NaOH. Furthermore, some  $\text{Al}_2\text{O}_3$  phases, such as corundum and spinel could be  
250 present in the sludge and would be insoluble [29].

251 In the elemental analysis high carbon content of 34.90 wt% has been identified in the original  
252 sludge, with smaller amounts of H (4.93 wt%) and N (0.60 wt%). The concentration of sulfur  
253 (0.66 wt%) quantified by elemental analysis is substantially lower than the one found by

1  
2  
3  
4 254 XRF. The high concentration reported in the XRF analysis may be due to the fact that its  
5  
6 255 analytical power is focused on the first layers of the sample. This implies that the  
7  
8 256 concentration of S is higher at the surface since the neutralizing substance ( $H_2SO_4$ ) acts on  
9  
10 257 the surface of the particle. Instead, in the elemental analysis, the complete combustion of the  
11  
12 258 sample is carried out, thus, the entire sulfur is oxidized to sulfur dioxide ( $SO_2$ ), which allows  
13  
14 259 quantifying the overall species [43]. Therefore, the S content provided by the elemental  
15  
16 260 analysis has been taken as the characterization reference value.

17  
18  
19  
20  
21  
22 261 Considering the results of ICP and elemental analysis, it can be concluded that the original  
23  
24 262 sludge is rich in carbon and aluminum (Table 2). The remaining species (25.18%) mainly  
25  
26 263 correspond to oxygen and traces of other metals. This implies that the metallic species have  
27  
28 264 been mostly oxidized. Moreover, in accordance with the concentrations of C, H, N, and S,  
29  
30 265 and considering the processes of the aluminum industry, it can be assumed that most of the  
31  
32 266 compounds present in the sludge are inorganic [44,45]. In view of these, in Table 2  
33  
34 267 summarizes the results for the overall mass balance of the main species identified in the raw  
35  
36 268 sludge (prior to extraction), determined by XRF, ICP, and elemental analyses.

37  
38  
39  
40  
41  
42 269 **Table 2.** Characterization of chemical properties of the raw sludge.

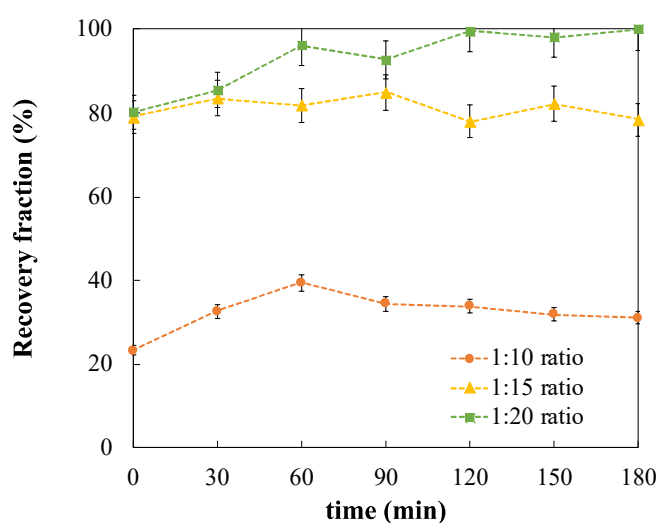
<b>Characterization</b>	
<b>Specie</b>	<b>Concentration [%wt.]</b>
Carbon	4.90
Aluminum	27.80
Oxygen*	55.18
Hydrogen	4.93
Silicon	3.48
Calcium	0.96
Sodium	0.94
Nitrogen	0.60
Sulfur	0.66
Iron	0.36
Nickel	0.16

Copper	0.04
* Obtained from the remaining balance	

270

271 *3.2. Extraction results*272 *3.2.1. Bayer method*

273 The results of the Bayer extraction throughout time are shown in Fig. 1, in which the recovery  
 274 fractions (RFs), defined in Eqs. (4) to (6), for different sludge/NaOH mass ratios are plotted.



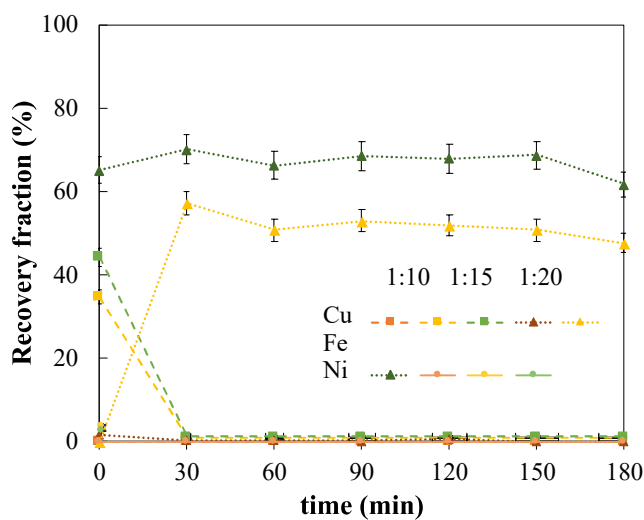
275

276 **Fig. 1.** Evolution of Al recovery fraction over time for different sludge/solution ratios during  
 277 the Bayer extraction.

278 Overall, an increase in the sludge/solution ratio gives way to higher RF values regardless of  
 279 the extraction time, being this effect more evident for an increase in the ratio from 1:10 to  
 280 1:15. However, at lower ratios, minor fluctuations are observed throughout time, due to a  
 281 more limited amount of extraction solution [27,28]. For a 1:20 ratio, the highest extraction  
 282 recovery fraction has been obtained, which shows an almost constant RF ~100% after 2 h.

283 Consequently, this ratio is the most suitable one in order to recover almost 100% of the Al  
 284 content from the raw sludge.

285 A selectivity test of the extraction method according to the recovery fraction obtained for  
 286 each compound has been performed and the results are shown in Fig. 2. This selectivity has  
 287 been calculated as the ratio between Al-RF and other metals RFs average. It should be noted  
 288 that the recovery fractions for Cu, Fe, and Ni are remarkably lower than that obtained for Al.  
 289 Hence, it can be affirmed that these species will be mainly concentrated in the solution during  
 290 the extraction process. This is mainly due to the electronegativity of the metals in question.  
 291 Al is the least electronegative species (1.61), therefore, its willingness to join other  
 292 complexes is greater than in the case of Fe (1.83), Cu (1.90), and Ni (1.91). Consequently,  
 293 the method is more selective towards Al [29].



294  
 295 **Fig. 2.** Recovery fraction of other metals over time and for different sludge/solution ratios  
 296 during the Bayer extraction.

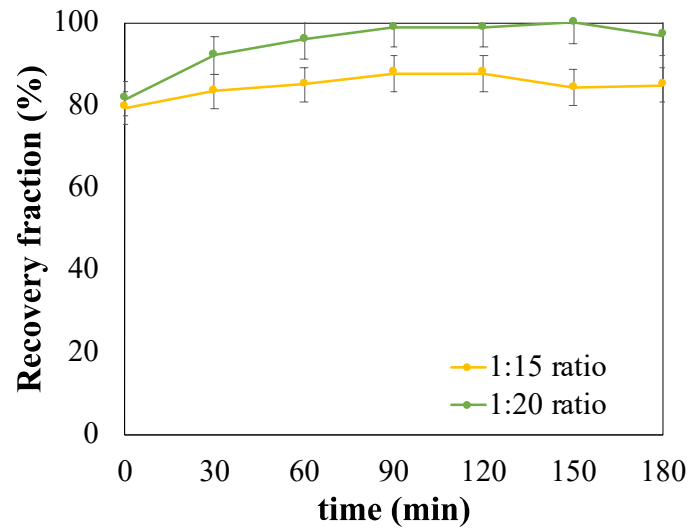
297 At zero-time, Ni extraction does not exceed 3% regardless the sludge/solution ratio used.  
 298 This could be attributed to the fact that Ni is a corrosion resistant species with caustic soda,



1  
2  
3  
4 299 therefore, it hardly occurs in the aqueous phase [46]. For Cu, at zero time and for 1:20 ratio  
5  
6 300 a fraction of 44% is recovered, while for the 1:15 ratio only 34% is recovered. This implies  
7  
8 301 that the full extraction has occurred during the first boil. During the complete extraction  
9  
10 302 process, its recovery varies between 0.99 and 1.26%, indicating that the extraction rate for  
11  
12 303 different ratios does not vary significantly. Ni shows a constant recovery, which implies that  
13  
14 304 the extraction occurred before boiling, similarly to Cu, without many differences between  
15  
16 305 ratios. Both species, Ni and Cu, show the higher electronegativity among the four species  
17  
18 306 analyzed. In the case of Fe, no extraction is observed for 1:10 ratio. The extraction using 1:15  
19  
20 307 ratio, shows a sharp increase in the recovery fraction up to 30 min, and then it remains almost  
21  
22 308 stable for a value of 0.5% average. The highest Fe recovery fraction is achieved (~63%) for  
23  
24 309 1:20 ratio, from the beginning of the extraction. Contrasting the Al RF data with the RF of  
25  
26 310 other metals, it is found that the 1:10 ratio has shown a better selectivity than the other ratios  
27  
28 311 studied. A small extraction of Ni, Fe, and Cu is observed (Fig. 2), which in some cases  
29  
30 312 reaches only up to 1%, while Al is up to almost 40% at 60 min. Therefore, the amounts of  
31  
32 313 Cu, Ni, and Fe that passes into the aqueous solution are not significant compared to the mass  
33  
34 314 of the extracted Al [47].  
35  
36  
37  
38  
39  
40  
41  
42

### 43 315 *3.2.2. HCl extraction*

44  
45  
46 316 In Fig. 3 the Al RFs are plotted for different sludge/solution ratios. Similarly, to the Bayer  
47  
48 317 process (NaOH extraction), the recovery fraction increases rapidly up to 90 mins and then  
49  
50 318 slowly approaches asymptotically to a constant a value. A similar behavior is observed for  
51  
52 319 both ratios. The highest recovery fraction (~100%) is attained for 1:20 ratio, which is  
53  
54 320 consistent with the availability of HCl in the solution.  
55  
56  
57  
58  
59  
60  
61  
62  
63  
64  
65



321

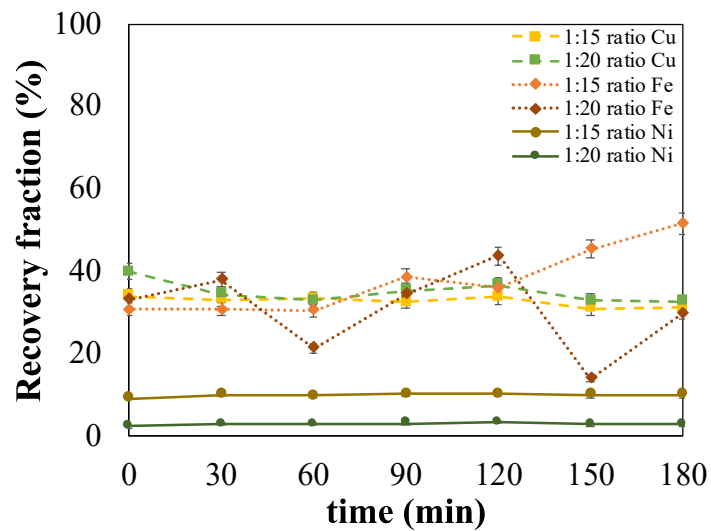
322 **Fig. 3.** Evolution of Al recovery fraction over time for different sludge/solution ratios

323 during the HCl extraction

324 Likewise, the RFs of the remaining metals are depicted in Fig. 4. In other studies, Al removal

325 efficiencies of up to approximately 96% have been reached. This study demonstrates that the

326 removal of Al by means of HCl is an alternative technique to the Bayer process [48,49].



327

328 **Fig. 4.** Recovery fraction of other metals over time and for different sludge/solution ratios

329 during the HCl extraction.

65

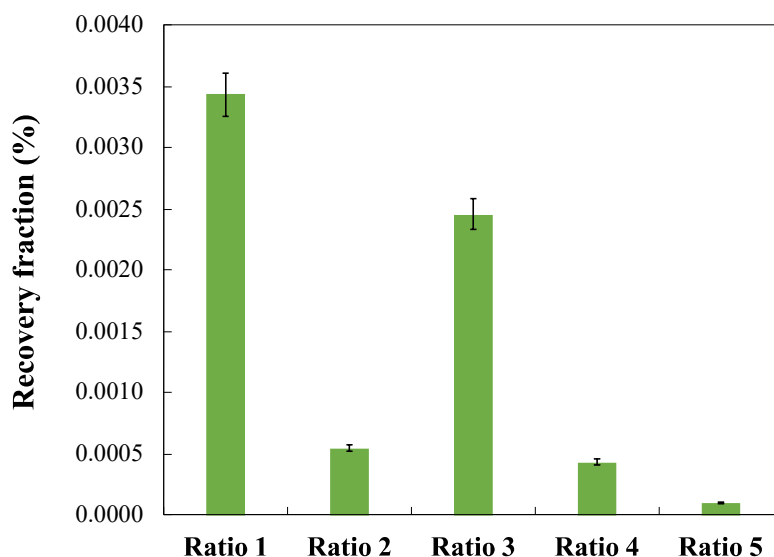
1  
2  
3  
4 330 Fig. 4 shows that the extraction with HCl is more selective than with NaOH in short times  
5  
6  
7 331 but at long times it is not very selective with respect to the other compounds present in the  
8  
9 332 sludge. The above, due the RF are less than 51% for Fe, 10% for Ni, and 40% for Cu. These  
10  
11 333 values are lower than those shown for NaOH (Fig. 2). The extraction of Cu and Fe is much  
12  
13 334 higher than the one for Ni. In the case of Cu, the maximum peak of extraction has been found  
14  
15  
16 335 with the 1:20 ratio at zero time, while for Fe this has been reached at 180 min with the 1:10  
17  
18 336 ratio. As with the NaOH extraction process, the extraction order has been the same, according  
19  
20  
21 337 to the electronegativity of the metals.

22  
23  
24 338 For Cu and Ni, similar stable behavior has been observed during the 180 min of extraction.  
25  
26 339 This may indicate that extraction has been occurred prior to boiling. Fe shows a different  
27  
28  
29 340 behavior, with variations during the 180 min of the process, but with more variations in the  
30  
31 341 1:20 ratio. Contrasting the Al RF data with the RF of Ni, Cu, and Fe, it has been found that  
32  
33  
34 342 despite the fact that both ratios present similar selectivity, 1:20 ratio shows a greater recovery  
35  
36 343 of Al with respect to the other metals. This is due to the fact that, for example, with the ratio  
37  
38  
39 344 1:15, there is a higher percentage of Ni present in the sample, while with a 1:20 ratio, it is  
40  
41 345 not. Also, it has been possible to consider for this study the 60<sup>th</sup> minute, as the best conditions  
42  
43  
44 346 for the extraction of Al; since Cu, Ni, and Fe show lower RFs, and an RF of approximately  
45  
46 347 95% is achieved for Al. Similarly, other studies have reported the high removal efficiency  
47  
48  
49 348 with HCl. They have also found that as the liquid-solid ratio increases there is no significant  
50  
51 349 improvement in the removal of Al [48–51].

### 52 53 54 350 *3.2.3. Isopropanol extraction*

55  
56  
57 351 Fig. 5 presents the RFs of each test. The RFs obtained are low, even the RF of the control  
58  
59  
60 352 performed is minor (4.56%). This can be attributed to the complex composition of the sludge,  
61  
62  
63  
64  
65

1  
2  
3  
4 353 shown in Table 2, in which different Al species are present. According to the Eq. (7), only  
5  
6 354 metallic Al will react with isopropanol, while in the case of HCl and NaOH more species  
7  
8  
9 355 react (Eqs. (1) - (3)), and, thus, higher recovery percentages are observed. Another factor is  
10  
11 356 the presence of water in the alcohol or in the reaction system, since aluminum isopropoxide  
12  
13 357 hydrolyzes to aluminum hydroxide in the presence of water [9].  $\text{Al}(\text{OH})_3$  is an insoluble white  
14  
15 358 compound [52], that it can be formed during the reaction, and then, can be easily mixed with  
16  
17 359 the remaining sludge. Since the system is not established under an inert atmosphere, the  
18  
19 360 humidity of the environment could hydrolyze the product. Also, the alcohol has not been  
20  
21 361 dried prior to the experiment, so any trace of water could favor this hydrolyzing too [53].  
22  
23  
24  
25  
26  
27  
28  
29  
30  
31  
32  
33  
34  
35  
36  
37  
38  
39  
40  
41  
42  
43  
44  
45



362

46  
47  
48 363 **Fig. 5.** Recovery fractions obtained by isopropanol extraction for different conditions  
49  
50  
51 364 (Table 1).  
52

53  
54 365 This is partly consistent with the results of the Al concentrations present in the sediment  
55  
56 366 of the Tests 4 and 5 (16% and 13.5%, respectively), since the mass of the hydroxyl group per  
57  
58 367 mole of Al is greater than that of the oxy group (2.1 times more weight). This implies that  
59  
60  
61  
62  
63  
64  
65

1  
2  
3  
4 368 the Al has been transformed from  $\text{Al}_2\text{O}_3$  to  $\text{Al}(\text{OH})_3$ , increasing the weight of the sediment  
5  
6 369 and decreasing the Al concentration of the solution. It is important to consider that  
7  
8  
9 370 isopropoxide is soluble in isopropanol, hence it has not been deposited on the sludge.  
10  
11 371 Additionally, its boiling point is about  $140\text{ }^\circ\text{C}$  at  $8.0258\text{ mmHg}$  [54], therefore, it was hardly  
12  
13  
14 372 dragged into the distillate during the distillation process.  
15

16  
17 373 Comparing the results, it can be perceived that an increase in time has not necessarily  
18  
19 374 improved the extraction. Tests 4 and 5, have been carried out for a duration of 11 h, which  
20  
21  
22 375 have shown the lowest extraction percentage; while the highest extraction has been obtained,  
23  
24 376 with those tests (Test 1 and 2) performed at 3 hours. In addition, higher recovery fractions  
25  
26  
27 377 have been obtained for lower amounts of catalyst ( $0.001\text{ mol mol}^{-1}\text{ Al}$ ). Furthermore, the  
28  
29 378 addition of  $\text{HgCl}_2$  has not significantly improved the extraction. For the Test 3, a good  
30  
31  
32 379 extraction is obtained using high amounts of catalyst, both  $\text{I}_2$  and  $\text{HgCl}_2$ , after 7 h.  
33

34  
35 380 The results with isopropanol have not been as expected, meanwhile, the extraction should  
36  
37 381 improve over time thus providing more energy and giving a long period for the formation of  
38  
39  
40 382 the desired compound. Also, the addition of more catalysts should enhance the reaction, to  
41  
42 383 break any oxide barrier so that the reaction can take place on the surface.  
43

### 44 384 3.2. *Comparison of the three extraction processes*

45  
46  
47  
48 385 In this study has only sought to compare the three extraction systems based on some  
49  
50  
51 386 assumptions. Therefore, it has been recommended for isopropanol extraction, to carry out  
52  
53 387 more tests and replicates to obtain specific statistical evidence to be able to conclude that this  
54  
55  
56 388 method is effective in removing Al. Another problem so that the isopropanol extraction was  
57  
58  
59  
60  
61  
62  
63  
64  
65

1  
2  
3  
4 389 not efficient has been the temperature used, which in other studies has shown that at high  
5  
6  
7 390 temperatures there is a greater formation of these aluminum gels [53,55].  
8

9  
10 391 HCl extraction has shown higher recovery percentages (+ 22.77% at 90 min) than the Bayer  
11  
12 392 process for short recovery times, but for longer times a similar recovery has been observed  
13  
14 393 in both treatments. This has possibly occurred due to the higher electronegativity of the  
15  
16 394 chloride ion compared to the electronegativity of the hydroxyl group. The Bayer method has  
17  
18 395 been more selective, since the extraction of Cu, Ni, and Fe is, on average, several times  
19  
20 396 greater in the extraction of HCl than in the Bayer process (Cu: 27 times greater, Fe: 3 times  
21  
22 397 greater, Ni: 17 times greater). In view of these results, the Bayer process for a 1:15 ratio  
23  
24 398 (BES15) has been the most selective extraction method and the samples recovered have  
25  
26 399 shown the highest Al content.  
27  
28  
29  
30  
31

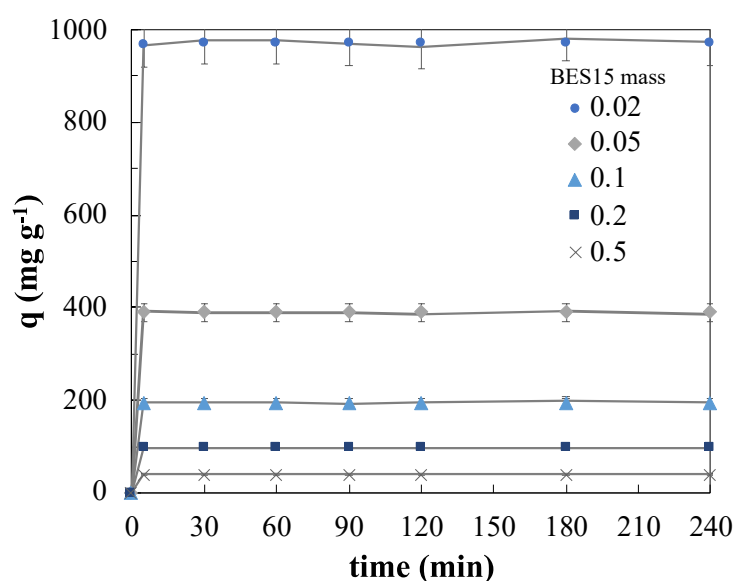
32 400 The obtained product (BES15) has been characterized by N<sub>2</sub> adsorption-desorption and TPD  
33  
34 401 of NH<sub>3</sub>, following the procedure described in Section 2.1. BES15 sample shows a BET  
35  
36 402 surface of 35.4 m<sup>2</sup> g<sup>-1</sup>, a microporous surface of 1.8 m<sup>2</sup> g<sup>-1</sup>, and mesopore volume of 0.14 cm<sup>3</sup>  
37  
38 403 g<sup>-1</sup>. The results are similar to those obtained in other works with BET surface areas of 32.9%  
39  
40 404 and 39.0 [56–58]. However, BES15 sample did not show any acidity. Hence, the BES15 has  
41  
42 405 been used as an adsorbent in the removal of CPS.  
43  
44  
45  
46  
47

### 48 406 *3.3. Chlorpyrifos removal from BES15 obtained by Al extracting*

49

50  
51 407 Fig. 6 shows the removal of CPS with the precipitate using BES15 as adsorbent (Eqs. (11)-  
52  
53 408 (12)). It can be observed that high removal rates are obtained after the initial contact of CPS  
54  
55 409 solution with BES15, by reaching a removal up to 96% after 5 mins of contact for all the  
56  
57  
58 410 weight ratios analyzed. Immediately, the CPS solution comes into contact with BES15. After,  
59  
60  
61  
62  
63  
64  
65

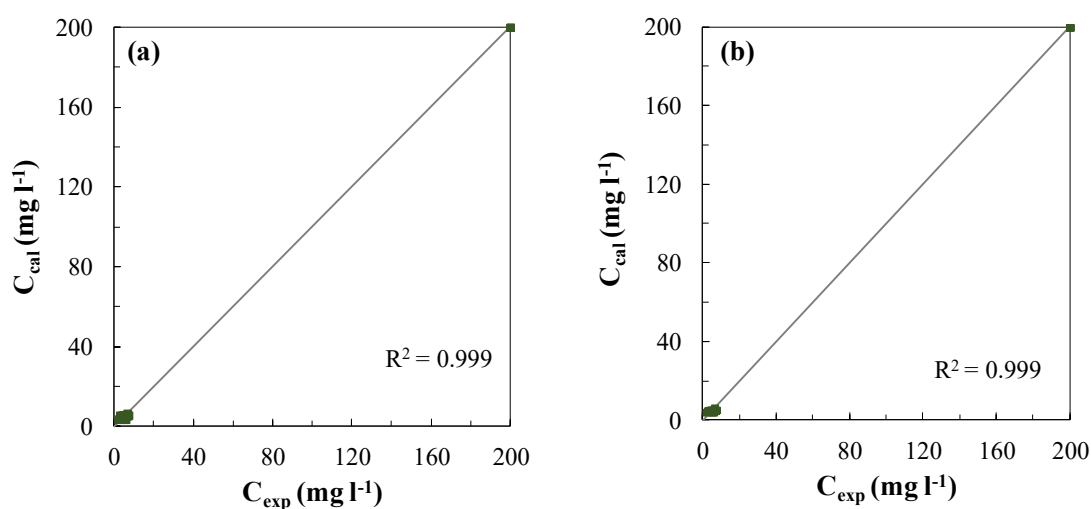
411 this behavior is kept constant throughout time, indicating that BES15 is a good adsorbent to  
 412 be used for the removal of organophosphate contaminants such as CPS. These results are  
 413 similar to those obtained in other studies published in the literature with CPS concentrations  
 414 between  $100 \mu\text{g l}^{-1}$  and  $500 \text{mg l}^{-1}$  [39,59–62]. The results of this study are better than those  
 415 found with other types of adsorbents, such as zinc oxide nanoparticles, which after 40 mins  
 416 of contact a removal of 70% was achieved [63]. It has been demonstrated that regardless the  
 417 amount of precipitate mass, high removal efficiencies have been achieved.



418  
 419 **Fig. 6.** CPS removal by BES15 synthesized adsorbent for different precipitated mass.  
 420 Operating conditions: 23 °C, 240 min.

421 Fig. 7 shows the parity graph corresponding to the two models used described in Section 2.3.  
 422 The values obtained in the fitting of the experimental data using the two adsorption models  
 423 are summarized in Table 5. Both models have been adjusted correctly, however, the  
 424 Langmuir model, which considers the formation of a single layer of adsorbate on the surface,  
 425 achieves the best adjustment for all the precipitated mass evaluated. Consequently, the *OF*

426 value of the Langmuir model ( $4.55 \cdot 10^{-22}$ ) is 12 orders of minor magnitude, in comparison to  
 427 the one obtained for the Freundlich model ( $1.72 \cdot 10^{-8}$ ). These results are not decisive to  
 428 conclude that the deposition of the CPS on the surface of BES15 could correspond to a  
 429 physical (physisorption) or chemical (chemisorption) mechanism, but they contribute a better  
 430 understanding of the process. Many authors argue that this mechanism cannot be assigned  
 431 based only on adequate kinetic models, but that different analytical techniques such as FTIR,  
 432 SEM, Raman spectroscopy, among others, must be performed. [36,64–66].



433 **Fig. 7.** Parity charts of the tested adsorption isotherm models. (a) Langmuir and (b)  
 434 Freundlich.

435 The value of  $K_L \alpha \rho_b$  (Table 5,  $1.06 \text{ min}^{-1}$ ) obtained for the Langmuir model is equal to that  
 436 found by Moussavi et al. [67] in the tests carried out with amoxicillin solutions of  $10 \text{ mg l}^{-1}$   
 437 on  $\text{NH}_4\text{Cl}$ -induced activated carbon. Several studies have been carried out for the removal of  
 438 CPS on zinc oxide nanoparticles and bagasse biochar, in which lower values ( $0.025 \text{ min}^{-1}$   
 439 and  $0.1205 \text{ min}^{-1}$ , respectively) were obtained [61,63].



440 **Table 5.** Balance parameters and mass transfer coefficient calculated for the models  
 441 evaluated

Parameter	Langmuir	Freundlich
$k_{La}\rho_b$ (min <sup>-1</sup> )	1.06	-
$OF$	$4.55 \cdot 10^{-22}$	$1.72 \cdot 10^{-8}$
$K_L$ (l mg <sup>-1</sup> )	8.23	
$q_m$ (mg g <sup>-1</sup> )	40.27	
$K_F$		1.53
$n$		0.45

442

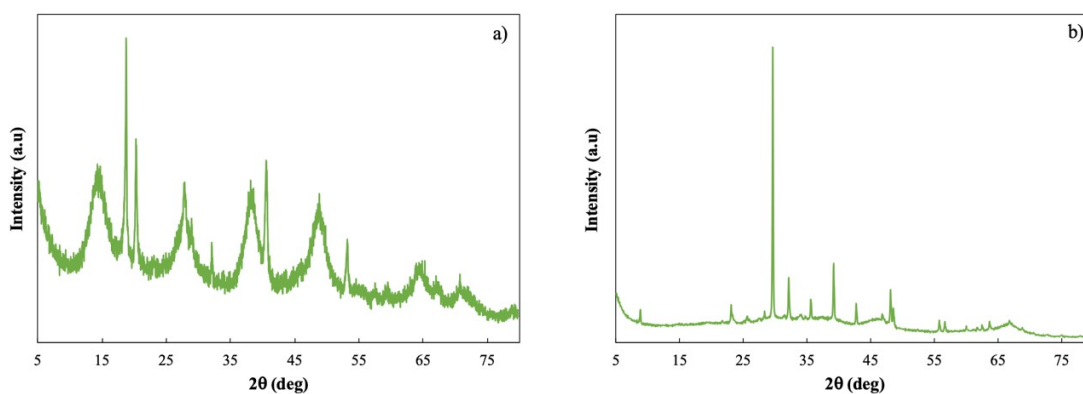
443 The value for  $q_m$  of 40.27 mg g<sup>-1</sup>, is similar to that found by ul Haq et al. [63] (47.85 mg g<sup>-1</sup>)  
 444 using zinc oxide nanoparticles, while this value is higher than that found by Jacob et al. [61]  
 445 (4.26 mg g<sup>-1</sup>) using bagasse biochar. In the case of  $K_F$ , 1.55 and 2.50 mg g<sup>-1</sup> were found,  
 446 similar to those found in this work.

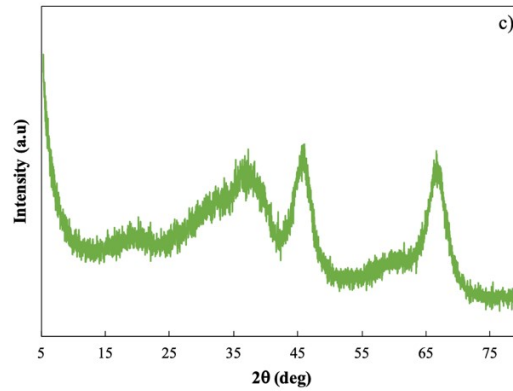
447 Therefore, the results obtained in our study on BES15 show good prospects, since this less  
 448 sophisticated adsorbent can be obtained as a by-product of the treatment of hazardous sludge  
 449 wastes derived from the metallurgical industry.

450 It must be considered that, according to European legislation, the individual concentrations  
 451 of this pollutant must not exceed 0.1 ppb. This work has been carried out for the removal of  
 452 a concentration of 200 ppm, which implies that BES15 could be used as a support in  
 453 conventional filtration systems due to its high removal rates.

454 *3.4. XRD and SEM Characterization*

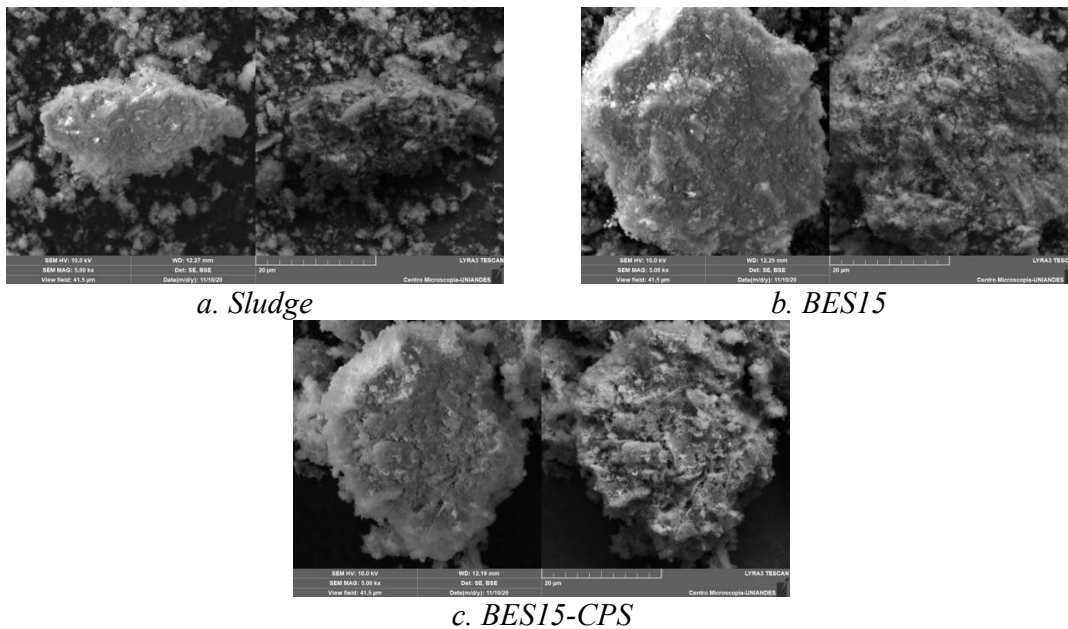
1  
2  
3  
4 455 In Fig. 8 it can be seen that after carrying out the Bayer process to the crude sludge, a  
5  
6 456 crystallinity of the material was achieved, thus showing that the Bayer process improves the  
7  
8  
9 457 sample's crystallinity. The above is reflected in the angle  $2\theta$  at  $29^\circ$  that corresponds to  
10  
11 458 aluminum. Furthermore, it is shown that after BES15 is used as an adsorbent, CPS  
12  
13  
14 459 considerably affects the crystallinity of the material, because it is adsorbed on the surface of  
15  
16 460 the material, thus verifying the results of the Langmuir model, which is also observed in the  
17  
18  
19 461 SEM images (Fig. 9c). This behavior is also observed in the increase in carbon on the surface  
20  
21 462 of the adsorbent after the CPS removal process (Table 6). In the XRD analyzes of the sludge,  
22  
23  
24 463 compounds such as boehmite, bichulite, calcite, calcium and bayerite were identified. In the  
25  
26 464 case of BES15, aluminum oxide was mainly identified at the angle  $2\theta$  at  $29^\circ$ . While for the  
27  
28  
29 465 BES15-CPS sample, aluminum oxide and other minor compounds such as carbon and  
30  
31 466 chlorine that can be associated with CPS were identified.  
32  
33





467 **Fig. 8.** XRD diagram of the evaluated samples. a) sludge, b) BES15 and c) BES15-CPS.

468 In Fig. 9 the SEM images are shown, it is observed that while the sludge there is little  
 469 consolidation and a typical sample of sludge from wastewater treatment is evident. After the  
 470 aluminum extraction process in the BES15 sample, a consolidation of the sample with  
 471 slightly more defined crystals and porosity in the sample was observed. Finally, after the  
 472 adsorption process, a layer is observed that can be attributed to the CPS carbon and that the  
 473 pores are saturated.



474 **Fig. 9.** SEM images of the different samples. a) sludge, b) BES15 and c) BES15-CPS.

475 Table 6 shows that in the sample of BES15-CPS there is the presence of compounds  
 476 associated with the removed insecticide such as chlorine and carbon (Fig. 8 and Fig. 9). While  
 477 the other minor CPS compounds are not detected by the equipment due to its low content and  
 478 the resolution of the equipment ( $> 0.1\%$ ).

479 With the EDS analysis it can be observed how after carrying out the aluminum extraction  
 480 process through the Bayer process the Na content increases considerably, because the  
 481 reaction of the process involves NaOH, then in the adsorption process it decreases  
 482 considerably. This behavior can be due to the fact that Na reacts and can be released in the  
 483 aqueous sample and leave as NaOH.

484 **Table 6.** Elemental content of the different samples (SEM-EDS)

Element	BES15 (Atomic %)	BES15 (Atomic %)	BES15-CPS (Atomic %)
C	6.81	-	9.53
O	67.46	0.24	51.25
F	1.28	3.44	2.94
Na	0.51	11.49	1.65
Al	23.70	27.64	33.89
Si	-	0.31	-
S	0.24	1.87	0.54
Cl	-	-	0.21
Total	100.00	100.00	100.00

485

#### 486 4. Conclusions

1  
2  
3  
4  
5  
6  
7  
8  
9  
10  
11  
12  
13  
14  
15  
16  
17  
18  
19  
20  
21  
22  
23  
24  
25  
26  
27  
28  
29  
30  
31  
32  
33  
34  
35  
36  
37  
38  
39  
40  
41  
42  
43  
44  
45  
46  
47  
48  
49  
50  
51  
52  
53  
54  
55  
56  
57  
58  
59  
60  
61  
62  
63  
64  
65

1  
2  
3  
4 487 In this work, we have successfully applied and compared three extraction methods for the  
5  
6 488 removal of Al from sludge wastes derived from the aluminum industry. It should be  
7  
8  
9 489 mentioned that these extraction methods have been scarcely investigated for the removal of  
10  
11 490 these types of wastes. Therefore, we have contributed to their suitable valorization in order  
12  
13  
14 491 to avoid an inappropriate disposal in landfills, by lessening their high environmental impact,  
15  
16 492 and by the proposal of an alternative application as adsorbents to remove CPS pollutants,  
17  
18  
19 493 which are widely used in agriculture, especially in developing countries.

20  
21  
22 494 Among the different Al extraction methods analyzed, the Bayer method has been the most  
23  
24 495 feasible one, especially for 1:15 and 1:20 sludge/NaOH ratios, where an Al recovery of 80%  
25  
26 496 and 100%, have been obtained, respectively. However, the selectivity for 1:20 ratio has been  
27  
28  
29 497 substantially lower than the one obtained for 1:15 ratio. In addition, an average recovery of  
30  
31  
32 498 60% iron, 40% copper, and 2.5% nickel have also been obtained with 1:20 ratio.

33  
34  
35 499 The Al extraction with HCl is also a feasible method. For a sludge/HCl ratio of 1:20 a stable  
36  
37 500 Al recovery of 99.32% has been achieved after 90 mins. However, this method is  
38  
39  
40 501 considerably less selective than the Bayer method. In this case, an average recovery of  
41  
42 502 34.56% of iron, 34.21% of copper and 6.54% of nickel have been obtained.

43  
44  
45 503 The Al extraction with isopropanol has not shown promising results, even when high  
46  
47 504 amounts of catalyst were added or HgCl<sub>2</sub> was used. Similarly, extraction was not improved  
48  
49  
50 505 over time. This could be attributed to the hydrolysis of the product to aluminum hydroxide,  
51  
52 506 as well as to its slow reaction rate and energy requirements.

53  
54  
55 507 Based on these results, the Al samples extracted by the Bayer method with a ratio of 1:15  
56  
57  
58 508 (BES15) have been tested for the CPS adsorption, in which a removal of 99% has been

1  
2  
3  
4 509 attained for 5 to 240 mins, by showing a stable performance, with no evidence of desorption.  
5

6  
7 510 A good fit has been established for the adsorption process, according to Langmuir isotherm,  
8

9 511 in which a single layer is formed at the beginning of the process.  
10

11  
12 512 The results shown above highlight the good prospects of these waste materials to be used as  
13

14 513 an economic adsorbent in filter columns. Furthermore, it must be considered that the CPS  
15

16 514 removal has been performed for higher concentration levels than those required by  
17

18  
19 515 legislation, which makes these results promising for its commercial application.  
20  
21

22  
23 516  
24  
25  
26  
27  
28  
29  
30  
31  
32  
33  
34  
35  
36  
37  
38  
39  
40  
41  
42  
43  
44  
45  
46  
47  
48  
49  
50  
51  
52  
53  
54  
55  
56  
57  
58  
59  
60  
61  
62  
63  
64  
65

1  
2  
3  
4 517 **AUTHOR INFORMATION**

5  
6  
7 518 **Corresponding author**

8  
9 519 Department of Civil and Environmental Engineering, Carrera 1Este #19A-40, Bogotá,  
10  
11 520 Colombia

12  
13 521 \*Tel.: +57 1 3394949 ext. 1649

14  
15  
16 522 E-mail: jf.saldarriaga@uniandes.edu.co or juanfelorza@gmail.com

17  
18 523 **CONFLICT OF INTEREST**

19  
20  
21 524 The authors declare no competing financial interest.

22  
23 525 **ACKNOWLEDGMENTS**

24  
25  
26 526 This work was carried out with financial support from the Department of Civil and Environmental  
27  
28 527 Engineering at Universidad de los Andes. Ministry of Economy and Competitiveness of the  
29  
30 528 Spanish Government (CTQ2016-77812-R and CTQ2016-79646-P), the ERDF funds and the  
31  
32  
33 529 Basque Government (Project IT1218-19). The authors thank the microscopy center  $\mu$ -core at  
34  
35  
36 530 the Universidad de los Andes.

37  
38  
39 531 **APPENDIX A. SUPPLEMENTARY DATA**

40  
41 532 Supplementary data file has been provided.  
42  
43  
44  
45  
46  
47  
48  
49  
50  
51  
52  
53  
54  
55  
56  
57  
58  
59  
60  
61  
62  
63  
64  
65

1  
2  
3  
4 **533 NOMENCLATURE**  
5  
6

7	534	$\alpha$	External surface area of adsorbent ( $\text{m}^2 \text{g}^{-1}$ )
8			
9			
10	535	$\rho_b$	Adsorbent bed density ( $\text{kg m}^{-3}$ )
11			
12			
13	536	$c_{cal}$	Values calculated by the model
14			
15			
16	537	$C_e$	Adsorbate concentration at equilibrium ( $\text{mg l}^{-1}$ )
17			
18			
19	538	$c_{exp}$	Phase measured experimentally
20			
21			
22	539	$C_i$	concentration of the aqueous phase at time I ( $\text{mg l}^{-1}$ )
23			
24			
25	540	$C_{sludge}$	initial sludge concentration (% wt)
26			
27			
28	541	$i$	sampling time
29			
30			
31	542	$k_I$	Rate constant of the PFO equation ( $\text{min}^{-1}$ )
32			
33			
34	543	$K_F$	Freundlich constant, ( $\text{mg g}^{-1}/(\text{mg l}^{-1})$ )
35			
36			
37	544	$K_L$	Constant related to the affinity between an adsorbent and adsorbate
38			
39	545		( $\text{l mg}^{-1}$ )
40			
41			
42	546	$k_L$	Mass transfer coefficient ( $\text{l m}^{-2} \text{min}^{-1}$ )
43			
44			
45	547	$K_L \alpha \rho_b$	represents the rate constant of the pseudo-first-order kinetic (PFO)
46			
47			
48	548		model
49			
50			
51	549	L	Volume of CPS solution (l)
52			
53			
54	550	$m_{sludge}$	initial sludge mass (g)
55			
56			
57	551	n	Freundlich intensity parameter(dimensionless)
58			
59			
60			
61			
62			
63			
64			
65			



1			
2			
3			
4	552	$Q^0_{\max}$	Maximum saturated monolater adsorption capacity of an adsorbent,
5			
6	553		( $\text{mg g}^{-1}$ )
7			
8			
9	554	$q_e, q_t$	Amounts of adsorbate uptake per mass of adsorbent at equilibrium
10			
11			
12	555	RF	Recovery fraction
13			
14			
15	556	$RF_i$	Recovery fraction at time i
16			
17			
18	557	$S_{\text{BET}}$	BET specific surface area ( $\text{m}^2 \text{g}^{-1}$ )
19			
20			
21	558	$S_i$	Product selectivity (%)
22			
23			
24	559	$S_{\text{micro}}$	Micropore area ( $\text{m}^2 \text{g}^{-1}$ )
25			
26			
27	560	t	Time (min)
28			
29			
30	561	$V_0$	initial volume (l)
31			
32			
33	562	$V_{al}$	aliquot volume (l)
34			
35			
36	563	$V_i$	Volume in the flask at time I (l)
37			
38			
39	564	$V_{\text{meso}}$	Mesopore volume ( $\text{cm}^3 \text{g}^{-1}$ )
40			
41			
42	565	$V_{\text{micro}}$	Micropore volume ( $\text{cm}^3 \text{g}^{-1}$ )
43			
44			
45	566	$V_p$	Pore volume ( $\text{cm}^3 \text{g}^{-1}$ )
46			
47			
48	567		
49			
50			
51	568		
52			
53			
54			
55			
56			
57			
58			
59			
60			
61			
62			
63			
64			
65			

569 **References**

- 570 [1] IAI, Primary aluminium production, Int. Alum. Inst. IAI. (2019). [http://www.world-](http://www.world-aluminium.org/statistics/primary-aluminium-production/)  
571 [aluminium.org/statistics/primary-aluminium-production/](http://www.world-aluminium.org/statistics/primary-aluminium-production/).
- 572 [2] D.V. Marques, R.L. Barcelos, G.O.C. Parma, E. Giroto, A.C. Júnior, N.C. Pereira, R.F.  
573 Magnago, Recycled polyethylene terephthalate and aluminum anodizing sludge-based  
574 boards with flame resistance, *Waste Manag.* 92 (2019) 1–14.  
575 <https://doi.org/10.1016/j.wasman.2019.05.013>.
- 576 [3] V. Mymrin, D.E. Pedroso, C. Pedroso, K. Alekseev, M.A. Avanci, E. Winter, L. Cechin,  
577 P.H.B. Rolim, A. Iarozinski, R.E. Catai, Environmentally clean composites with  
578 hazardous aluminum anodizing sludge, concrete waste, and lime production waste, *J.*  
579 *Clean. Prod.* 174 (2018) 380–388. <https://doi.org/10.1016/j.jclepro.2017.10.299>.
- 580 [4] Y. Zhang, M. Sun, J. Hong, X. Han, J. He, W. Shi, X. Li, Environmental footprint of  
581 aluminum production in China, *J. Clean. Prod.* 133 (2016) 1242–1251.  
582 <https://doi.org/10.1016/j.jclepro.2016.04.137>.
- 583 [5] C.G. Anderson, R.C. Dunne, J.L. Uhrig, *Mineral Processing and Extractive Metallurgy*,  
584 Society for Mining, Metallurgy & Exploration, Englewood, Colorado, 2014.
- 585 [6] H. Kvande, 3 - Production of primary aluminium, in: R. Lumley (Ed.), *Fundam. Alum.*  
586 *Metall.*, Woodhead Publishing, 2011: pp. 49–69.  
587 <https://doi.org/10.1533/9780857090256.1.49>.
- 588 [7] J.S. Saiz, G.C. Vargas, J.C.M. Piraján, Obtención de pseudoboehmita mediante el  
589 método de sol-gel empleando dos catalizadores diferentes, *Av. Investig. En Ing.* 1  
590 (2010) 35–44.

- 1  
2  
3  
4 591 [8] N. Louet, M. Gonon, G. Fantozzi, Influence of the amount of Na<sub>2</sub>O and SiO<sub>2</sub> on the  
5  
6 592 sintering behavior and on the microstructural evolution of a Bayer alumina powder,  
7  
8 593 Ceram. Int. 31 (2005) 981–987. <https://doi.org/10.1016/j.ceramint.2004.10.013>.
- 9  
10  
11 594 [9] O. Helmboldt, L.K. Hudson, C. Misra, K. Wefers, W. Heck, H. Stark, M. Danner, N.  
12  
13 595 Rösch, Aluminum Compounds, Inorganic, in: Ullmanns Encycl. Ind. Chem., American  
14  
15 596 Cancer Society, 2007: pp. 1–17. [https://doi.org/10.1002/14356007.a01\\_527.pub2](https://doi.org/10.1002/14356007.a01_527.pub2).
- 16  
17  
18 597 [10] W.G. Young, W.H. Hartung, F.S. Crossley, Reduction of Aldehydes with Aluminum  
19  
20 598 Isopropoxide<sup>1,2</sup>, J. Am. Chem. Soc. 58 (1936) 100–102.  
21  
22 599 <https://doi.org/10.1021/ja01292a033>.
- 23  
24  
25 600 [11] S.-J. Yoo, H.-S. Yoon, H.D. Jang, J.-W. Lee, S.-T. Hong, M.-J. Lee, S.-I. Lee, K.-W.  
26  
27 601 Jun, Synthesis of aluminum isopropoxide from aluminum dross, Korean J. Chem. Eng.  
28  
29 602 23 (2006) 683–687. <https://doi.org/10.1007/BF02706815>.
- 30  
31  
32 603 [12] S.O. Adeosun, O.I. Sekunowo, O.O. Taiwo, W.A. Ayoola, A. Machado, Physical and  
33  
34 604 Mechanical Properties of Aluminum Dross, Adv. Mater. 3 (2014) 6.  
35  
36 605 <https://doi.org/10.11648/j.am.20140302.11>.
- 37  
38  
39 606 [13] S. Elbasuney, Novel multi-component flame retardant system based on nanoscopic  
40  
41 607 aluminium-trihydroxide (ATH), Powder Technol. 305 (2017) 538–545.  
42  
43 608 <https://doi.org/10.1016/j.powtec.2016.10.038>.
- 44  
45  
46 609 [14] E. Álvarez-Ayuso, Approaches for the treatment of waste streams of the aluminium  
47  
48 610 anodising industry, J. Hazard. Mater. 164 (2009) 409–414.  
49  
50 611 <https://doi.org/10.1016/j.jhazmat.2008.08.054>.
- 51  
52  
53 612 [15] M.J. Ribeiro, J.A. Labrincha, Properties of sintered mullite and cordierite pressed  
54  
55 613 bodies manufactured using Al-rich anodising sludge, Ceram. Int. 34 (2008) 593–597.  
56  
57 614 <https://doi.org/10.1016/j.ceramint.2006.12.005>.
- 58  
59  
60  
61  
62  
63  
64  
65

- 1  
2  
3  
4 615 [16] S.-J. Park, M.-K. Seo, Chapter 6 - Element and Processing, in: S.-J. Park, M.-K. Seo  
5  
6 616 (Eds.), Interface Sci. Technol., Elsevier, 2011: pp. 431–499.  
7  
8 617 <https://doi.org/10.1016/B978-0-12-375049-5.00006-2>.
- 9  
10  
11 618 [17] F. Raupp-Pereira, D. Hotza, A.M. Segadães, J.A. Labrincha, Ceramic formulations  
12  
13 619 prepared with industrial wastes and natural sub-products, *Ceram. Int.* 32 (2006) 173–  
14  
15 620 179. <https://doi.org/10.1016/j.ceramint.2005.01.014>.
- 16  
17  
18 621 [18] U.S. EPA, EPA Method 3015A: Microwave Assisted Acid Digestion of Aqueous  
19  
20 622 Samples and Extracts, US EPA. (2007). [https://www.epa.gov/esam/epa-method-3015a-](https://www.epa.gov/esam/epa-method-3015a-microwave-assisted-acid-digestion-aqueous-samples-and-extracts)  
21  
22 623 [microwave-assisted-acid-digestion-aqueous-samples-and-extracts](https://www.epa.gov/esam/epa-method-3015a-microwave-assisted-acid-digestion-aqueous-samples-and-extracts) (accessed June 3,  
23  
24 624 2020).
- 25  
26  
27 625 [19] U.S. EPA, U.S. EPA Method 3051A: Microwave Assisted Acid Digestion of  
28  
29 626 Sediments, Sludges, and Oils, US EPA. (2007). [https://www.epa.gov/esam/us-epa-](https://www.epa.gov/esam/us-epa-method-3051a-microwave-assisted-acid-digestion-sediments-sludges-and-oils)  
30  
31 627 [method-3051a-microwave-assisted-acid-digestion-sediments-sludges-and-oils](https://www.epa.gov/esam/us-epa-method-3051a-microwave-assisted-acid-digestion-sediments-sludges-and-oils)  
32  
33 628 (accessed June 3, 2020).
- 34  
35  
36 629 [20] AWWA, 3120 metals by plasma emission spectroscopy (2017), in: *Stand. Methods*  
37  
38 630 *Exam. Water Wastewater*, American Public Health Association, 2018.  
39  
40 631 <https://doi.org/10.2105/SMWW.2882.047>.
- 41  
42  
43 632 [21] U.S. EPA, EPA Method 6010C (SW-846): Inductively Coupled Plasma - Atomic  
44  
45 633 Emission Spectrometry, (2007). [/homeland-security-research/epa-method-6010c-sw-](https://www.epa.gov/homeland-security-research/epa-method-6010c-sw-846-inductively-coupled-plasma-atomic-emission)  
46  
47 634 [846-inductively-coupled-plasma-atomic-emission](https://www.epa.gov/homeland-security-research/epa-method-6010c-sw-846-inductively-coupled-plasma-atomic-emission) (accessed June 3, 2020).
- 48  
49  
50 635 [22] K.A. Cychosz, R. Guillet-Nicolas, J. García-Martínez, M. Thommes, Recent advances  
51  
52 636 in the textural characterization of hierarchically structured nanoporous materials, *Chem.*  
53  
54 637 *Soc. Rev.* 46 (2017) 389–414. <https://doi.org/10.1039/C6CS00391E>.
- 55  
56  
57  
58  
59  
60  
61  
62  
63  
64  
65

- 1  
2  
3  
4 638 [23] M. Thommes, K. Kaneko, A.V. Neimark, J.P. Olivier, F. Rodriguez-Reinoso, J.  
5  
6 639 Rouquerol, K.S.W. Sing, Physisorption of gases, with special reference to the  
7  
8 640 evaluation of surface area and pore size distribution (IUPAC Technical Report), *Pure*  
9  
10  
11 641 *Appl. Chem.* 87 (2015) 1051–1069. <https://doi.org/10.1515/pac-2014-1117>.
- 12  
13 642 [24] A.T. Aguayo, A.G. Gayubo, R. Vivanco, M. Olazar, J. Bilbao, Role of acidity and  
14  
15 643 microporous structure in alternative catalysts for the transformation of methanol into  
16  
17 644 olefins, *Appl. Catal. Gen.* 283 (2005) 197–207.  
18  
19 645 <https://doi.org/10.1016/j.apcata.2005.01.006>.
- 20  
21 646 [25] H. Müller-Steinhagen, Determining silica solubility in bayer process liquor, *JOM.* 50  
22  
23 647 (1998) 44–49. <https://doi.org/10.1007/s11837-998-0286-6>.
- 24  
25 648 [26] S. Ostap, Control of Silica in the Bayer Process Used for Alumina Production, *Can.*  
26  
27 649 *Metall. Q.* 25 (1986) 101–106. <https://doi.org/10.1179/cmq.1986.25.2.101>.
- 28  
29 650 [27] W.J. Bruckard, J.T. Woodcock, Characterisation and treatment of Australian salt cakes  
30  
31 651 by aqueous leaching, *Miner. Eng.* 20 (2007) 1376–1390.  
32  
33 652 <https://doi.org/10.1016/j.mineng.2007.08.020>.
- 34  
35 653 [28] M. Davies, P. Smith, W.J. Bruckard, J.T. Woodcock, Treatment of salt cakes by  
36  
37 654 aqueous leaching and Bayer-type digestion, *Miner. Eng.* 21 (2008) 605–612.  
38  
39 655 <https://doi.org/10.1016/j.mineng.2007.12.001>.
- 40  
41 656 [29] M. Yoldi, E.G. Fuentes-Ordoñez, S.A. Korili, A. Gil, Efficient recovery of aluminum  
42  
43 657 from saline slag wastes, *Miner. Eng.* 140 (2019) 105884.  
44  
45 658 <https://doi.org/10.1016/j.mineng.2019.105884>.
- 46  
47 659 [30] A.D. Kelmers, R.M. Canon, B.Z. Egan, L.K. Felker, T.M. Gilliam, G. Jones, G.D.  
48  
49 660 Owen, F.G. Seeley, J.S. Watson, Chemistry of the direct acid leach, calssinter, and  
50  
51  
52  
53  
54  
55  
56  
57  
58  
59  
60  
61  
62  
63  
64  
65

- 1  
2  
3  
4 661 pressure digestion-acid leach methods for the recovery of alumina from fly ash, *Resour.*  
5  
6 662 *Conserv.* 9 (1982) 271–279. [https://doi.org/10.1016/0166-3097\(82\)90081-5](https://doi.org/10.1016/0166-3097(82)90081-5).  
7  
8  
9 663 [31] O. Mashtalir, M. Naguib, B. Dyatkin, Y. Gogotsi, M.W. Barsoum, Kinetics of  
10  
11 664 aluminum extraction from  $Ti_3AlC_2$  in hydrofluoric acid, *Mater. Chem. Phys.* 139  
12  
13 665 (2013) 147–152. <https://doi.org/10.1016/j.matchemphys.2013.01.008>.  
14  
15  
16 666 [32] R.S. Veerapur, K.B. Gudasi, T.M. Aminabhavi, Sodium alginate–magnesium  
17  
18 667 aluminum silicate mixed matrix membranes for pervaporation separation of water–  
19  
20 668 isopropanol mixtures, *Sep. Purif. Technol.* 59 (2008) 221–230.  
21  
22 669 <https://doi.org/10.1016/j.seppur.2007.06.005>.  
23  
24  
25  
26 670 [33] J.D. Seader, E.J. Henley, D.K. Roper, *Separation Process Principles*, 3rd Edition, John  
27  
28 671 Wiley Incorporated, 2010.  
29  
30  
31 672 [34] J.F. García-Reyes, B. Gilbert-López, A. Molina-Díaz, A.R. Fernández-Alba,  
32  
33 673 Determination of Pesticide Residues in Fruit-Based Soft Drinks, *Anal. Chem.* 80 (2008)  
34  
35 674 8966–8974. <https://doi.org/10.1021/ac8012708>.  
36  
37  
38 675 [35] L. Sharma, R. Kakkar, Magnetically retrievable one-pot fabrication of mesoporous  
39  
40 676 magnesium ferrite ( $MgFe_2O_4$ ) for the remediation of chlorpyrifos and real pesticide  
41  
42 677 wastewater, *J. Environ. Chem. Eng.* 6 (2018) 6891–6903.  
43  
44 678 <https://doi.org/10.1016/j.jece.2018.10.058>.  
45  
46  
47  
48 679 [36] H.N. Tran, S.-J. You, A. Hosseini-Bandegharai, H.-P. Chao, Mistakes and  
49  
50 680 inconsistencies regarding adsorption of contaminants from aqueous solutions: A critical  
51  
52 681 review, *Water Res.* 120 (2017) 88–116. <https://doi.org/10.1016/j.watres.2017.04.014>.  
53  
54  
55 682 [37] V.K. Gupta, A. Fakhri, S. Agarwal, N. Sadeghi, Synthesis of  $MnO_2$ /cellulose fiber  
56  
57 683 nanocomposites for rapid adsorption of insecticide compound and optimization by  
58  
59  
60  
61  
62  
63  
64  
65

- 1  
2  
3  
4 684 response surface methodology, *Int. J. Biol. Macromol.* 102 (2017) 840–846.  
5  
6 685 <https://doi.org/10.1016/j.ijbiomac.2017.04.075>.  
7  
8  
9 686 [38] M.R. Samarghandi, T.J. Al-Musawi, A. Mohseni-Bandpi, M. Zarrabi, Adsorption of  
10  
11 687 cephalixin from aqueous solution using natural zeolite and zeolite coated with  
12  
13 688 manganese oxide nanoparticles, *J. Mol. Liq.* 211 (2015) 431–441.  
14  
15 689 <https://doi.org/10.1016/j.molliq.2015.06.067>.  
16  
17  
18 690 [39] X.-Y. Tang, Y. Yang, M.B. McBride, R. Tao, Y.-N. Dai, X.-M. Zhang, Removal of  
19  
20 691 chlorpyrifos in recirculating vertical flow constructed wetlands with five wetland plant  
21  
22 692 species, *Chemosphere.* 216 (2019) 195–202.  
23  
24 693 <https://doi.org/10.1016/j.chemosphere.2018.10.150>.  
25  
26  
27 694 [40] L.K. Wang, J.P. Chen, Y. Hung, N.K. Shamma, *Heavy Metals in the Environment*, 1st  
28  
29 695 ed., CRC Press, Boca Raton, USA, 2009.  
30  
31  
32 696 [41] R. Galindo, I. Padilla, R. Sánchez-Hernández, J.I. Robla, G. Monrós, A. López-  
33  
34 697 Delgado, Production of added-value materials from a hazardous waste in the aluminium  
35  
36 698 tertiary industry: Synergistic effect between hydrotalcites and glasses, *J. Environ.*  
37  
38 699 *Chem. Eng.* 3 (2015) 2552–2559. <https://doi.org/10.1016/j.jece.2015.09.012>.  
39  
40  
41 700 [42] A. Gil, E. Arrieta, M.Á. Vicente, S.A. Korili, Application of Industrial Wastes from  
42  
43 701 Chemically Treated Aluminum Saline Slags as Adsorbents, *ACS Omega.* 3 (2018)  
44  
45 702 18275–18284. <https://doi.org/10.1021/acsomega.8b02397>.  
46  
47  
48 703 [43] W. Kirmse, *Organic Elemental Analysis: Ultramicro, Micro, and Trace Methods*,  
49  
50 704 Elsevier, London, UK, 2012.  
51  
52  
53 705 [44] E. Álvarez-Ayuso, H.W. Nugteren, Synthesis of dawsonite: A method to treat the  
54  
55 706 etching waste streams of the aluminium anodising industry, *Water Res.* 39 (2005) 2096–  
56  
57 707 2104. <https://doi.org/10.1016/j.watres.2005.03.017>.  
58  
59  
60  
61  
62  
63  
64  
65

- 1  
2  
3  
4 708 [45] P. Tansens, A.T. Rodal, C.M.M. Machado, H.M.V.M. Soares, Recycling of aluminum  
5  
6 709 and caustic soda solution from waste effluents generated during the cleaning of the  
7  
8 710 extruder matrixes of the aluminum industry, *J. Hazard. Mater.* 187 (2011) 459–465.  
9  
10 711 <https://doi.org/10.1016/j.jhazmat.2011.01.048>.  
11  
12  
13 712 [46] M. Yasuda, F. Takeya, F. Hine, Corrosion Behavior of Nickel in Concentrated NaOH  
14  
15 713 Solutions under Heat Transfer Conditions, *Corrosion.* 39 (1983) 399–405.  
16  
17 714 <https://doi.org/10.5006/1.3593879>.  
18  
19  
20 715 [47] M. Authier-Martin, G. Forte, S. Ostap, J. See, The mineralogy of bauxite for producing  
21  
22 716 smelter-grade alumina, *JOM.* 53 (2001) 36–40. [https://doi.org/10.1007/s11837-001-](https://doi.org/10.1007/s11837-001-0011-1)  
23  
24 717 0011-1.  
25  
26  
27 718 [48] Y. Huang, Z. Dou, T. Zhang, J. Liu, Leaching kinetics of rare earth elements and  
28  
29 719 fluoride from mixed rare earth concentrate after roasting with calcium hydroxide and  
30  
31 720 sodium hydroxide, *Hydrometallurgy.* 173 (2017) 15–21.  
32  
33 721 <https://doi.org/10.1016/j.hydromet.2017.07.004>.  
34  
35  
36 722 [49] S. Yang, K. Wei, W. Ma, K. Xie, J. Wu, Y. Lei, Kinetic mechanism of aluminum  
37  
38 723 removal from diamond wire saw powder in HCl solution, *J. Hazard. Mater.* 368 (2019)  
39  
40 724 1–9. <https://doi.org/10.1016/j.jhazmat.2019.01.020>.  
41  
42  
43 725 [50] I.T. Burke, C.L. Peacock, C.L. Lockwood, D.I. Stewart, R.J.G. Mortimer, M.B. Ward,  
44  
45 726 P. Renforth, K. Gruiz, W.M. Mayes, Behavior of Aluminum, Arsenic, and Vanadium  
46  
47 727 during the Neutralization of Red Mud Leachate by HCl, Gypsum, or Seawater, *Environ.*  
48  
49 728 *Sci. Technol.* 47 (2013) 6527–6535. <https://doi.org/10.1021/es4010834>.  
50  
51  
52 729 [51] Y. Liu, R. Naidu, Hidden values in bauxite residue (red mud): Recovery of metals,  
53  
54 730 *Waste Manag.* 34 (2014) 2662–2673. <https://doi.org/10.1016/j.wasman.2014.09.003>.  
55  
56  
57  
58  
59  
60  
61  
62  
63  
64  
65



- 1  
2  
3  
4 731 [52] PubChem, Aluminium hydroxide, (2005).  
5  
6  
7 732 <https://pubchem.ncbi.nlm.nih.gov/compound/6328211> (accessed June 3, 2020).  
8  
9 733 [53] L.S. Cividanes, T.M.B. Campos, L.A. Rodrigues, D.D. Brunelli, G.P. Thim, Review of  
10  
11 734 mullite synthesis routes by sol–gel method, *J. Sol-Gel Sci. Technol.* 55 (2010) 111–125.  
12  
13 735 <https://doi.org/10.1007/s10971-010-2222-9>.  
14  
15  
16 736 [54] J. Kijeński, R. Hombek, Step by Step Modeling of Superbasic Catalysts of the EDA  
17  
18 737 Complex Type, *J. Catal.* 167 (1997) 503–512. <https://doi.org/10.1006/jcat.1997.1561>.  
19  
20  
21 738 [55] K.G.K. Warriar, Sol-Gel Concepts as Applied to Alumina Ceramics, *Trans. Indian*  
22  
23 739 *Ceram. Soc.* 54 (1995) 144–148. <https://doi.org/10.1080/0371750X.1995.10804707>.  
24  
25  
26 740 [56] T.H. Boyer, A. Persaud, P. Banerjee, P. Palomino, Comparison of low-cost and  
27  
28 741 engineered materials for phosphorus removal from organic-rich surface water, *Water*  
29  
30 742 *Res.* 45 (2011) 4803–4814. <https://doi.org/10.1016/j.watres.2011.06.020>.  
31  
32  
33 743 [57] N. Maqbool, Z. Khan, A. Asghar, Reuse of alum sludge for phosphorus removal from  
34  
35 744 municipal wastewater, *Desalination Water Treat.* 57 (2016) 13246–13254.  
36  
37 745 <https://doi.org/10.1080/19443994.2015.1055806>.  
38  
39  
40 746 [58] L.Y. Wang, D.S. Tong, L.Z. Zhao, F.G. Liu, N. An, W.H. Yu, C.H. Zhou, Utilization  
41  
42 747 of alum sludge for producing aluminum hydroxide and layered double hydroxide,  
43  
44 748 *Ceram. Int.* 40 (2014) 15503–15514. <https://doi.org/10.1016/j.ceramint.2014.07.012>.  
45  
46  
47 749 [59] R.M. Agudelo, G. Peñuela, N.J. Aguirre, J. Morató, M.L. Jaramillo, Simultaneous  
48  
49 750 removal of chlorpyrifos and dissolved organic carbon using horizontal sub-surface flow  
50  
51 751 pilot wetlands, *Ecol. Eng.* 36 (2010) 1401–1408.  
52  
53 752 <https://doi.org/10.1016/j.ecoleng.2010.06.019>.  
54  
55  
56 753 [60] A. Huete-Soto, H. Castillo-González, M. Masís-Mora, J.S. Chin-Pampillo, C.E.  
57  
58 754 Rodríguez-Rodríguez, Effects of oxytetracycline on the performance and activity of  
59  
60  
61  
62  
63  
64  
65

- 1  
2  
3  
4 755 biomixtures: Removal of herbicides and mineralization of chlorpyrifos, *J. Hazard.*  
5  
6 756 *Mater.* 321 (2017) 1–8. <https://doi.org/10.1016/j.jhazmat.2016.08.078>.  
7  
8  
9 757 [61] M.M. Jacob, M. Ponnuchamy, A. Kapoor, P. Sivaraman, Bagasse based biochar for the  
10  
11 758 adsorptive removal of chlorpyrifos from contaminated water, *J. Environ. Chem. Eng.*  
12  
13 759 (2020) 103904. <https://doi.org/10.1016/j.jece.2020.103904>.  
14  
15  
16 760 [62] S. Vigneshwaran, J. Preethi, S. Meenakshi, Removal of chlorpyrifos, an insecticide  
17  
18 761 using metal free heterogeneous graphitic carbon nitride (g-C<sub>3</sub>N<sub>4</sub>) incorporated chitosan  
19  
20 762 as catalyst: Photocatalytic and adsorption studies, *Int. J. Biol. Macromol.* 132 (2019)  
21  
22 763 289–299. <https://doi.org/10.1016/j.ijbiomac.2019.03.071>.  
23  
24  
25  
26 764 [63] A. ul Haq, M. Saeed, M. Usman, S.A.R. Naqvi, T.H. Bokhari, T. Maqbool, H. Ghaus,  
27  
28 765 T. Tahir, H. Khalid, Sorption of chlorpyrifos onto zinc oxide nanoparticles impregnated  
29  
30 766 Pea peels (*Pisum sativum* L): Equilibrium, kinetic and thermodynamic studies, *Environ.*  
31  
32 767 *Technol. Innov.* 17 (2020) 100516. <https://doi.org/10.1016/j.eti.2019.100516>.  
33  
34  
35  
36 768 [64] E.C. Lima, A.R. Cestari, M.A. Adebayo, Comments on the paper: a critical review of  
37  
38 769 the applicability of Avrami fractional kinetic equation in adsorption-based water  
39  
40 770 treatment studies, *Desalination Water Treat.* 57 (2016) 19566–19571.  
41  
42 771 <https://doi.org/10.1080/19443994.2015.1095129>.  
43  
44  
45  
46 772 [65] E.C. Lima, M.A. Adebayo, F. Machado, Chapter 3. Kinetic and Equilibrium Models of  
47  
48 773 Adsorption, in: *Carbon Nanomater. Adsorbents Environ. Biol. Appl.*, Springer  
49  
50 774 International Publishing, New York, USA, 2015: pp. 33–70.  
51  
52  
53 775 [66] B. Volesky, Biosorption and me, *Water Res.* 41 (2007) 4017–4029.  
54  
55 776 <https://doi.org/10.1016/j.watres.2007.05.062>.  
56  
57  
58 777 [67] G. Moussavi, A. Alahabadi, K. Yaghmaeian, M. Eskandari, Preparation,  
59  
60 778 characterization and adsorption potential of the NH<sub>4</sub>Cl-induced activated carbon for the  
61  
62  
63  
64  
65

1  
2  
3  
4  
5  
6  
7  
8  
9  
10  
11  
12  
13  
14  
15  
16  
17  
18  
19  
20  
21  
22  
23  
24  
25  
26  
27  
28  
29  
30  
31  
32  
33  
34  
35  
36  
37  
38  
39  
40  
41  
42  
43  
44  
45  
46  
47  
48  
49  
50  
51  
52  
53  
54  
55  
56  
57  
58  
59  
60  
61  
62  
63  
64  
65

779 removal of amoxicillin antibiotic from water, Chem. Eng. J. 217 (2013) 119–128.  
780 <https://doi.org/10.1016/j.ccej.2012.11.069>.

781

782